JSHC
Japan Society of
Histochemistry and Cytochemistry
Established 1959

Acta Histochem. Cytochem. 55 (6): 185–192, 2022
doi: 10.1267/ahc.22-00032

*Regular Article*

# Immunohistochemical Localization of Alogliptin, a DPP-4 Inhibitor, in Tissues of Normal and Type 2 Diabetes Model Rat

**Yutaro Yamamoto, Kanae Ura, Takuma Matsukawa, Tetsuya Saita and Masashi Shin**

*Department of Applied Life Science, Faculty of Biotechnology and Life Science, Sojo University, 4–22–1 Ikeda, Nishi-ku, Kumamoto 860–0082, Japan*

Received March 29, 2022; accepted October 23, 2022; published online December 15, 2022

We investigated the pharmacokinetics of alogliptin (AG) at the cell and tissue level in healthy Wistar rats and a type 2 diabetic Goto-Kakizaki (GK) rat model. Immunohistochemistry of the renal tissue in these rats, post 1 hr of AG administration, showed that the signal was observed in the glomeruli, proximal tubule S3 segments, distal tubules, collecting ducts, and only in the brush border of the epithelial cells of the proximal tubule S1, S2 segments. After 6 hr of AG administration, the staining intensity of the regions other than the S3 segments was considerably reduced in Wistar rats, with no change observed in GK rats. At 24 hr, the staining intensity was considerably reduced, even in GK rats; however, the staining of the S3 segment remained unaltered in both. Hepatocytes in zone III of the hepatic lobule were more intensely stained than those in zone I in Wistar rats at 1 hr. However, almost no staining was observed in the hepatocytes of GK rats at 1 hr. Complete loss of signal was observed in the hepatocytes of the Wistar rats after 6 hr. This study revealed that the pharmacokinetics of AG in GK rats are different from those in Wistar rats.

**Key words:** alogliptin, immunohistochemistry, localization, Goto-Kakizaki (GK) rat

## I. Introduction

The number of diabetes patients worldwide has nearly tripled over the last 20 years and was estimated to be 436 million in 2019 [13]. Furthermore, an exponential rise is predicted in the number of diabetes patients, reaching 578 million by 2030, and 700 million by 2045 [13]. The prevalence of type 2 diabetes mellitus is high, accounting to 90–95% of the reported cases [25].

Therapeutic agents for type 2 diabetes include biguanides, thiazolidinediones, sulfonylureas, dipeptidyl peptidase-4 (DPP-4) inhibitors, α-glucosidase inhibitors, and sodium-glucose cotransporter 2 inhibitors. In Japan, DPP-4 inhibitors, such as alogliptin (AG), are used as first-line drugs in more than 65% of patients [3]. Compared to conventional drugs, DPP-4 inhibitors are considered to have a reduced risk of side effects, such as hypoglycemia and weight gain. Even so, understanding the detailed pharmacokinetics of these drugs will improve our understanding of the mechanisms underlying the function and the side effects, thereby aiding in the development of safer and more effective therapeutic use of drugs.

*In vivo* pharmacokinetics is an important parameter that affects the efficacy and side effects of drugs and is also related to their appropriate usage. However, pharmacokinetics mainly focuses on changes in plasma drug concentration, and little is known about the pharmacokinetics of drugs in cells and tissues, where many drugs act. Methods such as autoradiography and mass spectrometry imaging can be employed to analyze drug localization in cells and tissues. However, they cannot be performed easily because of the use of radioisotopes or the need for expensive equipment. As an alternative, we developed an "immunohistochemical detection method for drugs" and analyzed the localization of various drugs [9, 22, 28]. This method has advantages over autoradiography and mass spectrometry

Correspondence to: Masashi Shin, Department of Applied Life Science, Faculty of Biotechnology and Life Science, Sojo University, 4–22–1 Ikeda, Nishi-ku, Kumamoto 860–0082, Japan.
E-mail: mshin@life.sojo-u.ac.jp

© 2022 The Japan Society of Histochemistry and Cytochemistry

imaging as it facilitates safer, simpler, economical, and a more direct and precise evaluation of a drug localized in cells and tissues without the use of radioisotopes, radiation-controlled area, or expensive equipment.

We have previously reported on the preparation and characterization of a specific monoclonal antibody (mAb) against AG and the development of immunohistochemistry for its localization [26], and the pharmacokinetics of AG in the kidney and liver, which are the main organs involved in drug metabolism and excretion, in Wistar rats [27]. However, pharmacokinetics in diabetes patients may differ from those in the healthy population. Therefore, in this study, we aimed to compare the pharmacokinetics of AG in the kidney and liver of type 2 diabetic model and healthy rats.

## II. Materials and Methods

***Antibody***

Anti-AG mAb (AAG-78) was obtained as described previously [26]. This mAb has high specificity for AG but does not react with other drugs, such as sitagliptin, vancomycin, and amoxicillin [26].

***Animals***

Normal male Wistar rats (4–5 weeks old; CLEA Japan, Inc., Tokyo, Japan) weighing 180–200 g and diabetic male Goto-Kakizaki (GK) rats (4–5 weeks old; CLEA Japan, Inc., Tokyo, Japan) weighing 160–180 g were used. The GK rat, a model of type 2 diabetes mellitus, is characterized by insulin resistance and an insulin secretory defect. At the gestational age of 16.5 days, these rats exhibit a loss of pancreatic β-cell mass [4]. This strain was established by the selection of bred Wistar rats that exhibited glucose intolerance [11, 12]. This study was approved by the Animal Experiment Ethics Committee of Sojo University (approval number: 2021-L-006) and was performed in accordance with standard ethical guidelines for the care and use of laboratory animals [20]. The animals were housed in temperature- and light-controlled rooms (21 ± 1°C and 12:12 hr light-dark cycle) and had access to standard food and tap water *ad libitum*. A single dose of 5 mg AG/kg body weight was administered orally to both the strains (n = 9, Wistar; n = 9, GK). Three rats from each strain were used in the experiment at 1, 6, and 24 h after administration. At each time point, the rats were anesthetized with sodium pentobarbital (60 mg/kg; Abbott Laboratories, North Chicago, IL, USA) and transcardially perfused with phosphate-buffered saline (PBS) containing 5,000 IU of heparin sodium (AY Pharmaceuticals Co., Ltd., Tokyo, Japan) at 50 mL/min for 2 min at room temperature (20–25°C) and then with a freshly prepared solution of 2% glutaraldehyde in PBS for 6 min. Kidneys and liver were quickly excised from each rat and post-fixed in the same fixative for 5 hr at room temperature.

***Immunohistochemistry***

Immunohistochemical staining was performed as described previously [26, 27]. Post-fixed specimens were embedded in paraffin according to standard protocols. The samples were cut into 5-μm-thick sections, deparaffinized, and rehydrated. The sections were consecutively treated with (1) 6% hydrogen peroxide (Nacalai Tesque, Kyoto, Japan) in PBS for 30 min, (2) 2 N HCl for 30 min, (3) 0.03 mg/mL protease (Type XXIV: Bacterial; Sigma-Aldrich Co. Inc., St. Louis, MO, USA) in PBS for 60 min at 30°C and (4) 5 mg/mL $NaBH_4$ (Sigma-Aldrich Co. Inc., St. Louis, MO, USA) in PBS for 10 min. After each step, the specimens were washed thrice with PBS. Next, the specimens were blocked with a protein solution containing 10% normal goat serum, 1.0% bovine serum albumin (BSA), and 0.1% saponin in Tris-buffered saline (TBS) for 1 hr at room temperature and then directly incubated at 4°C overnight with AAG-78 mAb diluted 1:20 in TBS supplemented with 0.1% Triton X-100 (TBST). The sections were given three 5-min washes with TBST and then incubated with Simple Stain Rat MAX-PO (M) (Nichirei Bioscience Inc., Tokyo, Japan) for 2 hr at room temperature. After TBS rinses, the site of the antigen-antibody reaction was revealed using 3,3-diaminobenzidine tetrahydrochloride substrate (Dojindo Laboratories, Kumamoto, Japan) and $H_2O_2$ for 10 min.

Two types of negative control experiments were performed. One was a conventional control wherein the sections were exposed to normal mouse IgG diluted to 0.5 μg/mL with TBST instead of the primary mAb. The other was an absorption control in which an excessive amount of AG-*N*-(γ-maleimido-butyryloxy) succinimide (GMBS)-BSA conjugate (30 μg/mL) was added to the antibody solution before treating the sections.

***Semi-quantitative and statistical analysis of AG in rat kidney***

It is generally believed that the amount of antigen in cells and tissues correlates with the staining intensity of immunohistochemical staining. We measured the image density of kidney sections at each time point using ImageJ and performed a semi-quantitative analysis to examine changes in staining intensity. We took five low-magnification images of the upper region of renal cortex without the S3 segment of the proximal tubule per rat. Since the density value of each pixel in a digital image is 0 for black and 255 for white, the stronger (darker) the staining of the section, the smaller the density value. Therefore, the image density of each image was determined by subtracting the measured density value of the tissue from the value of an area without tissue in the section, such as from the lumen of a renal tubule or blood vessel. The average density of the five images was calculated and used as staining intensity of each rat. We then performed a t-test to determine whether there was a statistically significant difference in staining intensity between the rats of both strains at each time point. Statistical significance was set at $P < 0.05$.

## III. Results

### *Localization of alogliptin in rat kidney*

Alogliptin localization was assessed in the kidney. Immunohistochemical assessment in Wistar rats, 1 hr post AG administration, revealed varying degrees of staining in the renal cortex, with stronger signals observed in the lower region where the proximal tubule S3 segment was predominant (Figs. 1a, 2d). Moderate to intense staining was observed in the glomeruli. The epithelium of the distal tubules and collecting ducts exhibited both AG-positive as well as almost negative cells (Fig. 2a). In the proximal tubule S1 and S2 segments, moderate staining was observed only in the brush border of the epithelial cells, with no staining in the nucleus or cytoplasm (Fig. 2a). In the S3 segment, the brush border of the epithelial cells were also moderately stained; however, many of the nuclei were strongly stained, and the cytoplasm was weakly to moderately positive for AG (Fig. 2d). The staining pattern and intensity in the kidney of the GK rats was equivalent to that of the Wistar rats (Figs. 1e, 2e, h).

Though the staining intensity in different parts of the kidney reduced over time, the attenuation rates differed between Wistar and GK rats. In Wistar rats, the staining intensity in the glomeruli, proximal tubule S1 and S2 segments, distal tubules, and collecting ducts revealed a gradual decrease with a considerable reduction observed 6 hr after AG administration (Figs. 1b, 2b). However, in GK rats, staining intensities between 1 hr and 6 hr time points were not different (Figs. 1f, 2f). A statistically significant difference was observed in the staining intensity of the upper region of renal cortex between the two strains of rat at 6 hr after AG administration (Fig. 3).

The staining intensity in the upper region of renal cortex with glomeruli, proximal tubule S1 and S2 segments, distal tubules, and collecting ducts, was considerably reduced even in GK rats, 24 hr after administration, though it was marginally higher than that in Wistar rats (Fig. 2c, g). However, the staining in the lower region of the cortex with the proximal tubule S3 segment was similar to that seen at 1 hr, in both Wistar and GK rats (Fig. 1c, g).

### *Localization of alogliptin in rat liver*

In Wistar rats, the liver sections showed weak to intense staining 1 hr after AG administration (Fig. 4a). A differential staining intensity was observed in the region of the hepatic lobule and staining intensity of the hepatocytes in zone III (area around the central vein) was more than that of the hepatocytes in zone I (peripheral area of the hepatic lobule) (Fig. 4a, b, c). In zone III, the cytoplasm of hepatocytes was moderately positive, and many cells showed stronger nuclear staining (Fig. 4b). In addition, interlobular connective tissue, endothelial cells of the interlobular artery, interlobular vein, hepatic sinusoid, interlobular bile ducts, and Kupffer cells demonstrated moderate to intense staining (Fig. 4c). In contrast, the hepatocytes in GK rats, were barely stained, with no difference observed in the two zones (Fig. 4e, f, g). The staining pattern in the interlobular connective tissue, vascular endothelial cells, interlobular bile ducts, and Kupffer cells was similar to that observed in Wistar rats (Fig. 4f, g).

After 6 hr of AG administration, the staining intensity in the liver was considerably reduced in Wistar rats, showing a complete absence in the hepatocytes (Fig. 4d). In

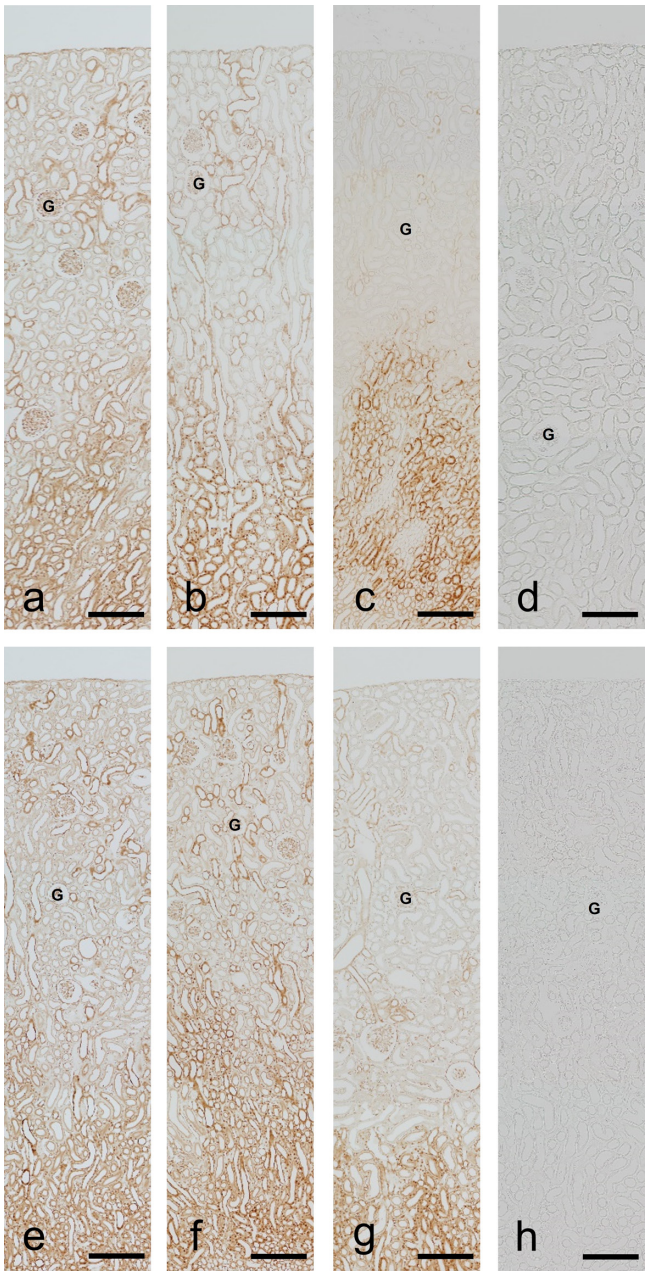


**Fig. 1.** Immunohistochemistry for AG in Wistar and GK rat kidney. Tissue samples are from Wistar rat (**a–d**) or GK rat (**e–h**) collected at 1 hr, (**a, d, e, h**), 6 hr (**b, f**) and 24 hr (**c, g**) after drug administration. **d**: Conventional control, **f**: Absorption control. G: glomerulus. Bars = 200 μm (**a–h**).

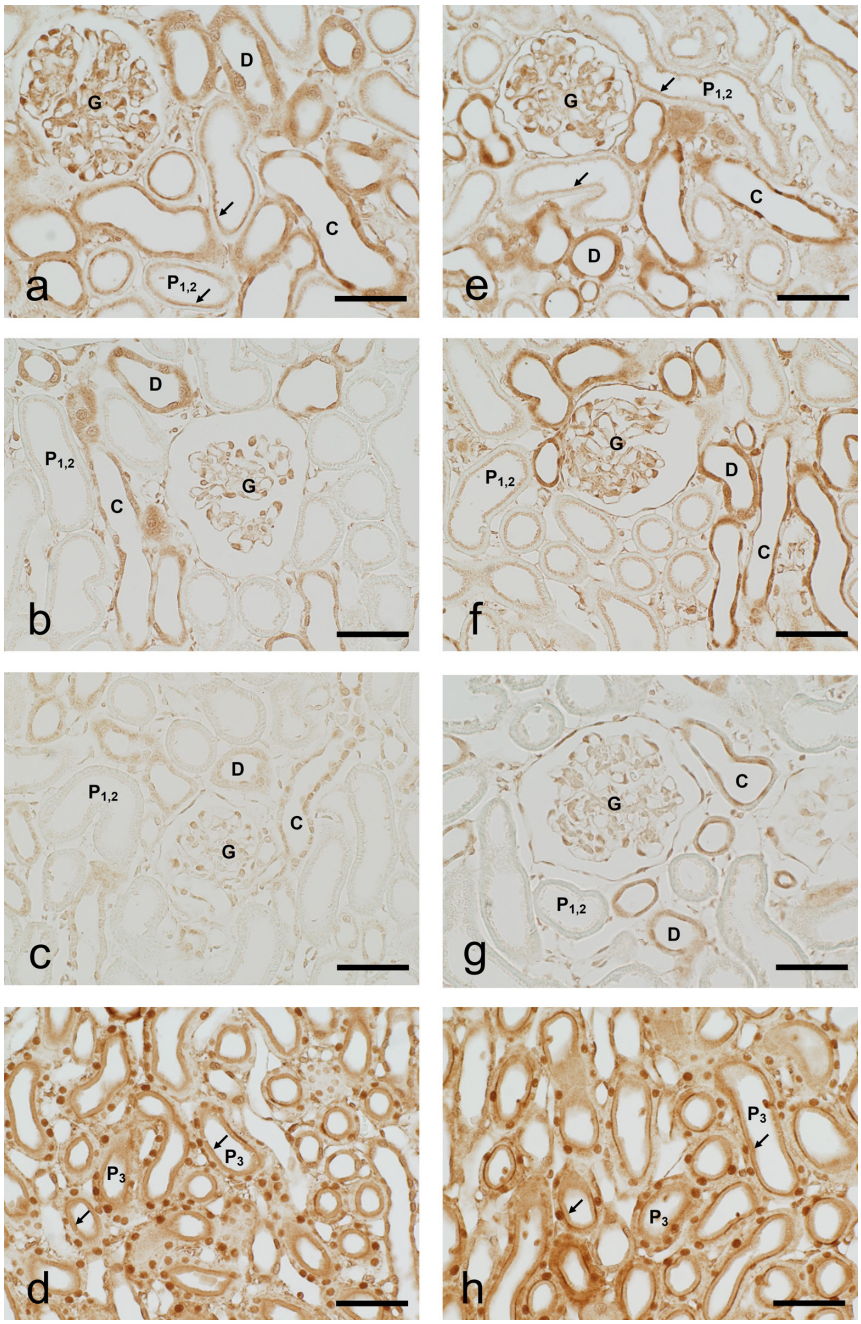


**Fig. 2.** High-magnification images of the renal cortex. Tissue samples from Wistar rat (**a–d**) or GK rat (**e–h**) and 1 hr (**a, d, e, h**), 6 hr (**b, f**) and 24 hr (**c, g**) after drug administration. **a–c, e–g**: upper region, **d, h**: lower region, G: glomerulus, $P_{1,2}$: $S_1$ or $S_2$ segment of proximal tubules, $P_3$: $S_3$ segment of proximal tubules, D: distal tubules, C: collecting ducts, arrows: brush border. Bars = 50 μm (**a–f**).

addition, the staining intensity in the interlobular connective tissue and the hepatic triad was greatly attenuated, in both Wistar as well as GK rats (Fig. 4d, h). No staining was observed in the liver at the 24 hr time point in both Wistar and GK rats (data not shown).

***Negative control experiments***

The conventional immunohistochemical staining controls demonstrated no staining for AG (Fig. 1d). The absorption controls showed that the addition of AG-GMBS-BSA at a concentration of 30 μg/mL to the primary antibody solution abolished all staining (Fig. 1h).

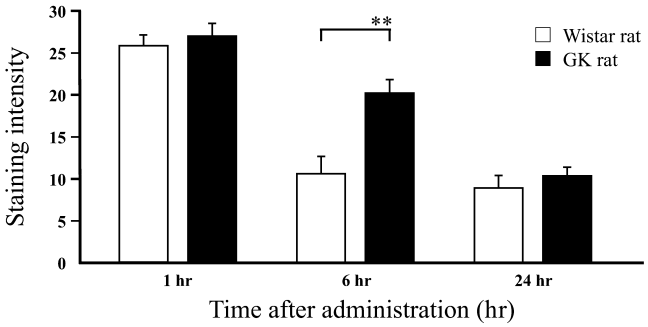


**Fig. 3.** Change in staining intensity over time in the upper region of renal cortex of Wistar and GK rats. Data are presented as mean ± SD (n = 3). ** $P < 0.01$.

## IV. Discussion

Immunohistochemistry requires rapid fixation, as slow fixation increases the possibility of antigen migration from *in situ*. Glutaraldehyde, which is essential for drug immunohistochemistry, has a high crosslinking activity, but it also has poor tissue permeability. Therefore, we performed perfusion fixation for rapid fixation. However, in perfusion fixation, the perfusion pressure may also cause antigen migration. However, we previously reported that AG staining was stronger in hepatocytes in zone III (downstream, low perfusion pressure) than that in zone I (upstream, high perfusion pressure) [27], suggesting that drug relocation due to perfusion pressure is unlikely. Therefore, we

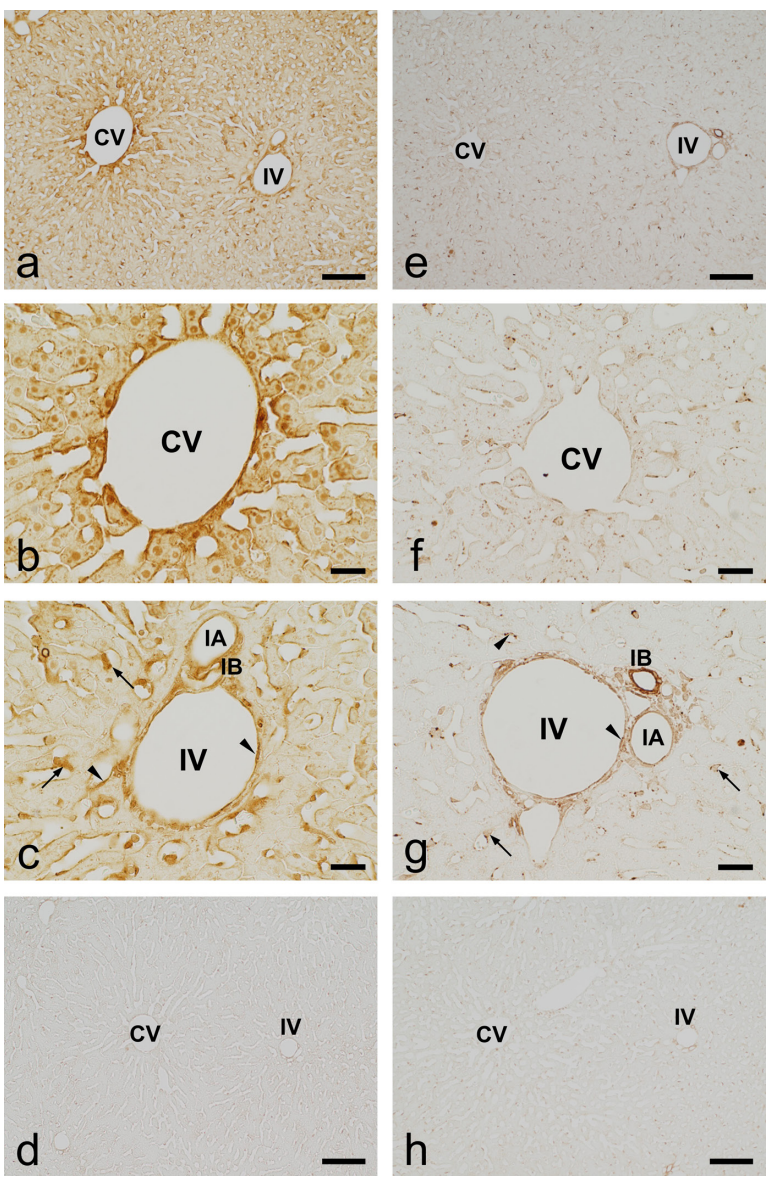


**Fig. 4.** Immunohistochemistry for AG in liver tissue from Wistar and GK rat liver. Tissue samples are from Wistar rat (**a–d**) or GK rat (**e–h**) collected at 1 hr (**a–c, e–g**) or 6 hr (**d, h**) after drug administration. CV: central vein, IV: interlobular vein, IA: interlobular artery, IB: interlobular bile duct, arrows: Kupffer cells, arrow heads: endothelial cells. Bars = 100 μm (**a, d, e, h**); 25 μm (**b, c, f, g**).

believe that the localization of AG obtained in this study is accurate.

The immunohistochemical staining intensity depends on the amount of antigen present in the cells/section. When an antigen is a drug, the amount of intracellular drug is estimated as the difference between the amount of drug taken up by the cell and that excreted from the cell. The mechanisms for the uptake and excretion of drugs across cell membranes include simple diffusion and transporter-mediated transport. AG has a molecular weight of 339.39 and a low lipophilicity (log P = −1.4) [18], which makes it difficult to pass through the cell membrane by simple diffusion. This suggests the involvement of transporters.

To the best of our knowledge, only one report by Morimoto *et al.* suggests the involvement of transporters for AG, which mentions that although AG is a cationic drug, AG uptake into Caco-2 cells was significantly inhibited by the organic anion transporting polypeptide (OATP) substrate and by the OATP inhibitor, but was not inhibited by organic cation transporter (OCT), organic cation/carnitine transporter (OCTN), or peptide transporter 1 (PEPT1) substrates [18].

Drug excretion from the kidneys is determined by the balance between glomerular filtration, tubular reabsorption, and tubular secretion. Therefore, immunostaining of tubular epithelial cells is believed to represent the difference between drug reabsorption from primary urine and drug secretion. Proximal tubular epithelial cells express several transporters that are involved in drug reabsorption from primary urine (PEPT1, PEPT2, organic anion transporter 2 (OAT2), and OAT4 [5, 6, 14, 20]), and drug secretion (OAT1, OAT2, OAT3, OCT2 for uptake from the basolateral side [2, 14], P-glycoprotein (P-gp), multidrug resistance protein 2 (MRP2), MRP4, and breast cancer resistance protein (BCRP) for secretion to tubular lumen [2, 8, 14]). Excretion transporters such as P-gp (apical side) and 190-kD MRP (basolateral side) are expressed in distal tubules and collecting ducts [7, 10, 19], while, as for uptake transporters, OAT2 (apical side) and OAT3 (basolateral side) are expressed in the collecting ducts [15].

The basement membrane, which plays a major role in glomerular filtration, is negatively charged and is a physical filter that does not allow molecules with a diameter of 10 nm or more to pass through. It also acts as a charge-selective barrier for the negatively charged molecules. As AG is a cationic drug with a small molecular weight, it easily passes through the basement membrane, and most of it is filtered into primary urine. Among the reabsorption transporters present on the apical side of proximal tubular epithelial cells, PEPTs do not use AG as a substrate and OAT2 and OAT4 could possibly use AG as a substrate, but OAT4 is not expressed in rats [21, 29].

In both Wistar and GK rats, the epithelial cells of the proximal tubule S1 and S2 segments were not stained, except for the brush border, 1 hr after AG administration. Therefore, the reabsorption by OAT2 was negligible, and AG in the primary urine was considered to be hardly reabsorbed. We believe that the staining of the brush border is due to the binding of AG to DPP-4 on the cell membrane and not the uptake process because DPP-4 is expressed in the proximal tubule epithelial cells [1, 17].

Excretory transporters such as P-gp, MRP2, MRP4, and BCRP are expressed on the apical side of the proximal tubular epithelial cells [2, 8, 29]. P-gp is also expressed in distal tubules and collecting ducts [7, 10]. However, we believe that these transporters rarely secrete AG from epithelial cells into the primary urine because AG is excreted in urine and not in bile, though P-gp, MRP2, and BCRP are also expressed in the bile canaliculi membrane of hepatocytes [16]. Therefore, AG in tubular epithelial cells is taken up from the basolateral side, and the difference in the staining intensity of the cells at each site is considered to be due to the difference in the expression level of uptake transporters, such as OAT1 and OAT3, in each cell. There are no reports on OATs expression at any site of the nephron; however, our results suggest that they are abundantly expressed in the S3 segment of the proximal tubule and moderately expressed in some cells of the distal tubule and collecting duct. AG taken up into cells might be excreted slowly into the primary urine or transferred to the blood via MRP2, MRP4, or without transporters.

The localization and staining pattern of AG in GK rats were similar to that of Wistar rats, but the rate of signal attenuation in the distal tubules and collecting ducts was reduced, and moderate-to-strong staining remained at 6 hr after administration. As discussed above, we believe that AG is rarely secreted from the epithelial cells into primary urine via the excretion transporters such as P-gp, MRP2, MRP4, and BCRP, thereby suggesting that the uptake of AG at these sites may have increased in GK rats. Previous reports have shown the changes in the expression of transporter mRNAs (downregulation: OCT1, OCTN2, OATP2B1, and OATP1A5; upregulation: OAT2, MRP4, and BCRP) in the kidneys of rats with type 2 diabetes induced by a high-fat diet and streptozotocin [24]. Though there are no reports of altered transporter expression in GK rats, increased expression of excretion transporters is unlikely to affect pharmacokinetics. Therefore, the slower attenuation of staining intensity in these sites in GK rats may be attributed to the increased expression of organic anion uptake transporters such as OATs.

In Wistar rat liver 1 hr post AG administration, the staining intensity of hepatocytes was different in the region of the hepatic lobule and zone III hepatocytes showed stronger staining than zone I hepatocytes. As mentioned above, AG does not easily pass through the cell membrane by simple diffusion, so we believed that the transporters are involved in the uptake and excretion of the drug. In hepatocytes, the excretion transporters P-gp, MRP2, and BCRP are localized on the bile canaliculi (a part of the apical cell membrane of hepatocytes) [16, 23], while the uptake transporters (OAT2, OATP1B1, OATP1B3, OATP2B1, and

OCT1) and the excretion transporters (MRP3, MRP4, and MRP6) are located on the basolateral side [16]. There have been no reports on the expression of transporters in each zone. However, stronger staining in zone III hepatocytes may indicate that the uptake transporters such as OAT2 and OATPs are highly expressed in zone III hepatocytes. AG, which is known to be rapidly excreted from the kidney, accumulated in hepatocytes 1 hr after drug administration. Since, it is unclear whether AG is metabolized or detoxified in the liver, the meaning of this accumulation is for future work. In addition, though the excretion of AG in the bile has not been shown, hepatocyte staining almost disappeared after 6 hr. This suggests that intracellular drugs are returned to the blood by MRPs within a few hours of administration.

In GK rats, hepatocyte staining was not observed post 1 hr of drug administration. Wang *et al.* reported that the mRNA expression levels of OAT2, OATP2B1, and OATP1A5 were decreased, whereas those of OCTN2, OATP3A1, OATP1A1, and MDR2 were increased in the liver of streptozotocin-induced type 2 diabetic rats [24]. Therefore, we presume that the expression of OATs and/or OATPs is decreased in GK rats, and that drug uptake into hepatocytes is suppressed.

This study revealed that the pharmacokinetics of AG at the cell and tissue level in type 2 diabetes model GK rats was different from that in healthy Wistar rats. This variation may be due to the increased expression of transporters that take up organic anions into cells, such as OATs and OATPs, in the kidney and decreased expression in the liver of GK rats, which needs to be assessed in future. Researches using healthy animals are important for basic understanding. Furthermore, comparative studies with healthy animals and pathological animal models aid in a better understanding of the pharmacokinetics at the cell and tissue level.

## V. Conflicts of Interest

The authors declare no conflicts of interest.

## VI. Acknowledgment

We would like to thank Editage (www.editage.com) for English language editing.

## VII. References

1. Ariyoshi, M., Mizuno, M., Morisue, Y., Shimada, M., Fujita, S., Nasu, J., *et al.* (2002) Identification of a target antigen recognized by a mouse monoclonal antibody to the bile canalicular surface of rat hepatocytes with a random phage display library. *Acta Med. Okayama* 56; 187–191.
2. Basit, A., Radi, Z., Vaidya, V. S., Karasu, M. and Prasad, B. (2019) Kidney Cortical Transporter Expression across Species Using Quantitative Proteomics. *Drug Metab. Dispos.* 47; 802–808.
3. Bouchi, R., Sugiyama, T., Goto, A., Imai, K., Ihana-Sugiyama, N., Ohsugi, M., *et al.* (2021) Retrospective nationwide study on the trends in first-line antidiabetic medication for patients with type 2 diabetes in Japan. *J. Diabetes Investig.* 13; 280–291.
4. Bourgneuf, C., Bailbé, D., Lamazière, A., Dupont, C., Moldes, M., Farabos, D., *et al.* (2021) The Goto-Kakizaki rat is a spontaneous prototypical rodent model of polycystic ovary syndrome. *Nat. Commun.* 12; 1064.
5. Brandsch, M. (2009) Transport of drugs by proton-coupled transporters: pearls and pitfalls. *Expert Opin. Drug Metab. Toxicol.* 5; 887–905.
6. Ekaratanawong, S., Anzai, N., Jutabha, P., Miyazaki, H., Noshiro, R., Takeda, M., *et al.* (2004) Human organic anion transporter 4 is a renal apical organic anion/dicarboxylate exchanger in the proximal tubules. *J. Pharmacol. Sci.* 94; 297–304.
7. Ernest, S., Rajaraman, S., Megyesi, J. and Bello-Reuss, E. N. (1997) Expression of MDR1 (multidrug resistance) gene and its protein in normal human kidney. *Nephron* 77; 284–289.
8. Fallon, J. K., Smith, P. C., Xia, C. Q. and Kim, M. S. (2016) Quantification of Four Efflux Drug Transporters in Liver and Kidney across Species Using Targeted Quantitative Proteomics by Isotope Dilution NanoLC-MS/MS. *Pharm. Res.* 33; 2280–2288.
9. Fujiwara, K., Shin, M., Miyazaki, T. and Maruta. Y. (2011) Immunocytochemistry for amoxicillin and its use for studying uptake of the drug in the intestine, liver, and kidney of rats. *Antimicrob. Agents Chemother.* 55; 62–71.
10. Ginn, P. E. (1996) Immunohistochemical detection of P-glycoprotein in formalin-fixed and paraffin-embedded normal and neoplastic canine tissues. *Vet. Pathol.* 33; 533–541.
11. Goto, Y., Kakizaki, M. and Masaki, N. (1976) Production of spontaneous diabetic rats by repetition of selective breeding. *Tohoku J. Exp. Med.* 119; 85–90.
12. Guest, P. C. (2019) Characterization of the Goto-Kakizaki (GK) Rat Model of Type 2 Diabetes. *Methods Mol. Biol.* 1916; 203–211.
13. International Diabetes Federation (2019) IDF Diabetes Atlas (9th edition), pp. 33–34.
14. Inui, K., Masuda, S. and Saito, H. (2000) Cellular and molecular aspects of drug transport in the kidney. *Kidney Int.* 58; 944–958.
15. Kojima, R., Sekine, T., Kawachi, M., Cha, S. H., Suzuki, Y. and Endou, H. (2002) Immunolocalization of Multispecific Organic Anion Transporters, OAT1, OAT2, and OAT3, in Rat Kidney. *J. Am. Soc. Nephrol.* 13; 848–857.
16. Maeda, K. (2010) Transporters involved in hepatobiliary transport of drugs. *Folia Pharmacol. Jpn.* 135; 76–79.
17. Mentzel, S., Dijkman, H. B., Van Son, J. P., Koene, R. A. and Assmann, K. J. (1996) Organ distribution of aminopeptidase A and dipeptidyl peptidase IV in normal mice. *J. Histochem. Cytochem.* 44; 445–461.
18. Morimoto, K., Sasaki, M., Oikawa, E., Abe, M., Kikuchi, T., Ishii, M., *et al.* (2021) Intestinal Absorption of Alogliptin Is Mediated by a Fruit-Juice-Sensitive Transporter. *Biol. Pharm. Bull.* 44; 653–658.
19. Peng, K. C., Cluzeaud, F., Bens, M., Duong Van Huyen, J. P., Wioland, M. A., Lacave, R., *et al.* (1999) Tissue and Cell Distribution of the Multidrug Resistance-Associated Protein (MRP) in Mouse Intestine and Kidney. *J. Histochem. Cytochem.* 47; 757–767.
20. Science Council of Japan (2006) Guidelines for Proper Conduct of Animal Experiments.
21. Shen, H., Liu, T., Morse, B. L., Zhao, Y., Zhang, Y., Qui, X., *et al.* (2015) Characterization of Organic Anion Transporter 2 (SLC22A7): A Highly Efficient Transporter for Creatinine and

Species-Dependent Renal Tubular Expression. *Drug Metab. Dispos.* 43; 984–493.
22. Shin, M., Larsson, L.-I., Hougaard, D. M. and Fujiwara, K. (2009) Daunomycin accumulation and induction of programmed cell death in rat hair follicles. *Cell Tissue Res.* 337; 429–438.
23. Tydén, E., Tallkvist, J., Tjälve, H. and Larsson, P. (2008) P-glycoprotein in intestines, liver, kidney and lymphocytes in horse. *J. Vet. Pharmacol. Ther.* 32; 167–176.
24. Wang, J., Zhai, T. and Chen, Y. (2018) Effects of Honokiol on CYP450 Activity and Transporter mRNA Expression in Type 2 Diabetic Rats. *Int. J. Mol. Sci.* 19; 815.
25. WHO (2016) Global Report on Diabetes, World Health Organization, Geneva.
26. Yamamoto, Y., Yamamoto, Y., Saita, T. and Shin, M. (2019) Immunohistochemistry for anti-diabetes drug, alogliptin using a newly prepared monoclonal antibody: Its precise localization in rat small intestine. *Acta Histochem. Cytochem.* 52; 27–34.
27. Yamamoto, Y., Yamamoto, Y., Saita, T., Hira, D., Chijiwa, T. and Shin, M. (2020) Immunohistochemical pharmacokinetics of the anti-diabetes drug alogliptin in rat kidney and liver. *Acta Histochem. Cytochem.* 53; 55–60.
28. Yamamoto, Y., Yamamoto, Y., Saita, T. and Shin, M. (2021) Immunohistochemical localization and pharmacokinetics of the anti-MRSA drug teicoplanin in rat kidney using a newly developed specific antibody. *Med. Mol. Morphol.* 54; 227–236.
29. Zou, W., Shi, B., Zeng, T., Zhang, Y., Huang, B., Ouyang, B., *et al.* (2021) Drug Transporters in the Kidney: Perspectives on Species Differences, Disease Status, and Molecular Docking. *Front. Pharmacol.* 12; 746208

This is an open access article distributed under the Creative Commons Attribution-NonCommercial 4.0 International License (CC-BY-NC), which permits use, distribution and reproduction of the articles in any medium provided that the original work is properly cited and is not used for commercial purposes.